THE JOURNAL OF BIOLOGICAL CHEMISTRY Vol. 277, No. 42, Issue of October 18, pp. 39554–39560, 2002
Printed in U.S.A.

Subcellular Targeting and Agonist-induced Site-specific Phosphorylation of Endothelial Nitric-oxide Synthase*

Received for publication, July 19, 2002, and in revised form, August 8, 2002
Published, JBC Papers in Press, August 19, 2002, DOI 10.1074/jbc.M207299200

Eva Gonzalez‡§, Ruqin Kou‡, Alison J. Lin¶‖, David E. Golan¶, and Thomas Michel‡**‡‡**

From the ‡Cardiovascular and ¶Hematology Divisions, Brigham and Women's Hospital, Department of Biological Chemistry and Molecular Pharmacology, Harvard Medical School, Boston, Massachusetts 02115 and the ‡‡Veterans Affairs Boston Healthcare System, West Roxbury, Massachusetts 02132

The endothelial isoform of nitric-oxide synthase (eNOS) undergoes a complex pattern of covalent modifications, including acylation with the fatty acids myristate and palmitate as well as phosphorylation on multiple sites. eNOS acylation is a key determinant for the reversible subcellular targeting of the enzyme to plasmalemmal caveolae. We transfected a series of hemagglutinin epitope-tagged eNOS mutant cDNAs deficient in palmitoylation (palm$^-$) and/or myristoylation (myr$^-$) into bovine aortic endothelial cells; after treatment with the eNOS agonists sphingosine 1-phosphate or vascular endothelial growth factor, the recombinant eNOS was immunoprecipitated using an antibody directed against the epitope tag, and patterns of eNOS phosphorylation were analyzed in immunoblots probed with phosphorylation state-specific eNOS antibodies. The wild-type eNOS underwent agonist-induced phosphorylation at serine 1179 (a putative site for phosphorylation by kinase Akt), but phosphorylation of the myr$^-$ eNOS at this residue was nearly abrogated; the palm$^-$ eNOS exhibited an intermediate phenotype. The addition of the CD8 transmembrane domain to the amino terminus of eNOS acylation-deficient mutants rescued the wild-type phenotype of robust agonist-induced serine 1179 phosphorylation. Thus, membrane targeting, but not necessarily acylation, is the critical determinant for agonist-promoted eNOS phosphorylation at serine 1179. In striking contrast to serine 1179, phosphorylation of eNOS at serine 116 was enhanced in the myr$^-$ eNOS mutant and was markedly attenuated in the CD8-eNOS membrane-targeted fusion protein. We conclude that eNOS targeting differentially affects eNOS phosphorylation at distinct sites in the protein and suggest that the inter-relationships of eNOS acylation and phosphorylation may modulate eNOS localization and activity and thereby influence NO signaling pathways in the vessel wall.

The endothelial isoform of nitric-oxide synthase (eNOS)[1] plays a major role in the control of vascular homeostasis and platelet aggregation (1, 2). In vascular endothelial cells and in cardiac myocytes, eNOS is targeted to signal-transducing microdomains in the plasma membrane termed caveolae, where eNOS interacts with the scaffolding protein caveolin (for review, see Ref. 3). Plasmalemmal caveolae serve as membrane sites of sequestration of signaling proteins including receptors, G proteins, and protein kinases as well as eNOS (for review, see Ref. 4). The targeting of eNOS to the membrane is mediated by dual acylation, an irreversible *N*-myristoylation at Gly^2, and reversible thiopalmitoylation at Cys^{15} and Cys^{26} (5). Mutagenesis of the eNOS myristoylation site blocks both myristoylation and palmitoylation and converts the membrane-targeted wild-type eNOS to a soluble protein; the myr$^-$ mutant is recovered in the soluble subcellular fraction when expressed in cells (6, 7). The palmitoylation-deficient mutant eNOS (palm$^-$) exhibits an intermediate phenotype; the palm$^-$ mutant does undergo myristoylation, and its membrane association is only partially reduced compared with the wild-type eNOS (5). The addition of a prototypical transmembrane domain to the myr$^-$ eNOS is sufficient to promote eNOS palmitoylation as well as targeting to caveolae (8) and also restores agonist responsiveness of the acylation-deficient mutant eNOS enzyme (9). Taken together, these results suggest that the caveolar location and functionality of eNOS are determined by structural features of the eNOS molecule that are distinct from the enzyme sites of acylation (10, 11).

Acylation is not the only covalent modification that importantly affects eNOS. Like the other NOS isoforms, eNOS is a phosphoprotein (12). There are at least three distinct eNOS phosphorylation sites: serine 116 (13, 14), threonine 497 (threonine 495 in the human sequence (15)), and serine 1179 (serine 1177 in the human sequence (13, 16, 17)). Of these phosphorylation sites, the one most extensively characterized is serine 1179. Several distinct serine/threonine protein kinases have been implicated in the cellular activation of eNOS by promoting phosphorylation at serine 1179, including kinase Akt (16, 17) and the AMP-activated protein kinase (18) as well as protein kinase A (19). eNOS phosphorylation at serine 1179 has been observed in response to a wide variety of extracellular stimuli, including treatment of endothelial cells with vascular endothelial growth factor (VEGF) (16, 20), sphingosine-1-phos-

* This work was supported in part by National Institutes of Health Grants HL46457 and GM36259 (to T. M.) and HL32854 and HL15157 (to D. E. G.). The costs of publication of this article were defrayed in part by the payment of page charges. This article must therefore be hereby marked "*advertisement*" in accordance with 18 U.S.C. Section 1734 solely to indicate this fact.

§ Recipient of a Fulbright Postdoctoral Research Fellowship.

‖ Supported by National Institutes of Health Training Grant T32ES07155.

** To whom correspondence should be addressed: Cardiovascular Division, Brigham and Women's Hospital, 75 Francis St., Boston, MA 02115. Tel.: 617-732-7376; Fax: 617-732-5132; E-mail: michel@calvin.bwh.harvard.edu (to T. M.) or Dept. of Biological Chemistry and Molecular Pharmacology, Harvard Medical School, 250 Longwood Ave., Boston, MA 02115. Tel.: 617-432-2256; Fax: 617-432-3833; E-mail: dgolan@hms.harvard.edu (to D. E. G.).

[1] The abbreviations used are: eNOS, endothelial nitric-oxide synthase; S1P, sphingosine 1-phosphate; VEGF, vascular endothelial growth factor; HA, hemagglutinin; BAEC, bovine aortic endothelial cells; myr-eNOS, mutant eNOS in which the myristoylation site at glycine 2 is changed to alanine rendering the enzyme acylation-deficient; palm-eNOS, mutant eNOS in which the palmitoylation sites at cysteines 15 and 26 are changed to serine; EGFP, enhanced green fluorescent protein; MOPS, 4-morpholinepropanesulfonic acid.

phate (S1P) (21), insulin (22), lysophosphatidic acid (23), or estrogens (24) as well as fluid shear stress (13, 17). Agonist-induced dephosphorylations involving threonine 497 (15, 25) and serine 116 (14) have also been observed. The pathways involved in agonist-specific modulation of these distinct phosphorylation sites remain under active investigation, and the inter-relationships between eNOS acylation and phosphorylation are incompletely understood.

In the present study, we have analyzed the role of eNOS targeting in the regulation of enzyme phosphorylation. We studied the phosphorylation patterns of a series of hemagglutinin (HA) epitope-tagged eNOS acylation mutants in which the myristoylation and/or palmitoylation sites had been inactivated by site-directed mutagenesis. We analyzed these constructs in transient transfection experiments performed in bovine aortic endothelial cells (BAEC), thereby avoiding the potential confounding effects of cell-specific phosphorylation pathways. To distinguish the recombinant eNOS constructs from the native enzyme expressed in BAEC, we immunoprecipitated the recombinant protein using an antibody against the HA epitope tag. Using a series of phosphorylation state-specific antibodies, we were able to show that distinct eNOS phosphorylation sites are differentially affected by altering the subcellular targeting of the protein.

EXPERIMENTAL PROCEDURES

Materials—Fetal bovine serum was purchased from Hyclone (Logan, UT). Cell culture reagents and media were from Invitrogen. FuGENE 6 transfection reagent was from Roche Molecular Biochemicals. S1P was purchased from BioMol (Plymouth Meeting, PA). VEGF and wortmannin were from Calbiochem. Anti-phospho-Ser^{1179}-eNOS antibody, anti-phospho-Akt antibody (serine 473), and anti-Akt antibody were from Cell Signaling Technologies (Beverly, MA). Anti-phospho-Ser^{116}-eNOS was from Upstate Biotechnology, Inc. (Lake Placid, NY). Anti-eNOS monoclonal antibody was from Transduction Laboratories (Lexington, KY). Monoclonal antibody 12CA5 directed against the HA epitope was from Roche Molecular Biochemicals. Anti-HA epitope polyclonal antibody was from Santa Cruz Biotechnology. Protein G-Sepharose beads were from Zymed Laboratories Inc. (South San Francisco, CA). Purified recombinant kinase Akt was from Upstate Biotechnology, Inc. (Lake Placid, NY). Super Signal substrate for chemiluminescence detection and secondary antibodies conjugated with horseradish peroxidase were from Pierce. Tris-buffered saline and phosphate-buffered saline were purchased from Boston Bioproducts (Ashland, MA). Other reagents were from Sigma.

Plasmid Construction—cDNA constructs encoding the HA-tagged wild-type eNOS, myristoylation-deficient eNOS (myr$^-$ eNOS; Gly^2 mutated to Ala), palmitoylation-deficient eNOS (palm$^-$ eNOS; Cys^{15} and Cys^{26} mutated to Ser), and Akt phosphorylation site-deficient mutant (Ser^{1179} mutated to Ala) have been previously described (5, 26). Chimeric cDNA constructs encoding the fusion proteins CD8.myr$^-$ eNOS and CD8.myr$^-$ palm$^-$ eNOS have also been described (8). The HA epitope tag was added to these various CD8.eNOS chimeras by interchanging the untagged 3′-terminal 1.5 kilobases of these constructs with the corresponding HA epitope-tagged eNOS cDNA, taking advantage of a propitious *Bgl*II restriction site.

For cell imaging studies, we constructed a series of eNOS fusion proteins with the fluorescent protein EGFP; our preliminary studies had revealed that the constructs tagged with the HA epitope yielded a signal-to-noise ratio that was insufficient for high resolution fluorescence imaging. The plasmid encoding the eNOS-EGFP fusion protein was made by cloning the cDNA encoding the sequence of bovine wild-type eNOS into the mammalian expression vector pEGFP-N1 (Clontech Laboratories, Inc., Palo Alto, CA) after first modifying the stop codon at the 3′ end of the eNOS sequence by using PCR-based mutagenesis to generate a *Bam*HI restriction site; the stop codon was then used to clone the eNOS sequence in-frame with the EGFP sequence. To produce palm$^-$ eNOS-EGFP, CD8·myr$^-$ eNOS-EGFP, and CD8·myr$^-$ palm$^-$ eNOS-EGFP, these cDNAs were digested with *Eco*RI and *Kpn*I, and the 5′ fragment was use to replace the corresponding region in the wild-type eNOS-EGFP plasmid that had been similarly digested to release the corresponding 5′ fragment. To construct myr$^-$ eNOS-EGFP, the CD8·myr$^-$ eNOS was first digested with *Cla*I, blunted with mung bean nuclease, and digested with *Kpn*I; this cDNA fragment was subcloned into eNOS-EGFP that had been first digested with *Nhe*I, blunted with mung bean nuclease, and digested with *Kpn*I to release the 5′ fragment that was then replaced by the myr$^-$ sequence.

Cell Culture, Transfection, and Drug Treatment—Bovine aortic endothelial cells were obtained from Cell Systems (Kirkland, WA) and maintained in culture in Dulbecco's modified Eagle's medium supplemented with fetal bovine serum (10% v/v) as described (12). Cells were plated onto gelatin-coated culture dishes and studied before cell confluence between passages 5 and 9. BAEC in 60-mm dishes were transfected with plasmids encoding wild-type eNOS, eNOS mutants, and chimeric constructs using FuGENE 6 (following the supplier's instructions) and were analyzed 48 h after transfection. The culture medium was changed to serum-free medium, and incubation proceeded overnight before all experiments were conducted (21, 27); transfection frequency using these conditions was ~35%.

S1P was solubilized in methanol and stored at −20 °C; the same volume of methanol was used as vehicle control, and the final concentration of methanol did not exceed 0.4% (v/v). VEGF was solubilized in Tris-buffered saline containing 0.1% bovine serum albumin and stored at −70 °C. Wortmannin was solubilized in dimethyl sulfoxide and kept at −20 °C; where indicated dimethyl sulfoxide 0.1% (v/v) was used as vehicle control.

Preparation of Cellular Lysates, Immunoprecipitation, and Immunoblotting—After drug treatments, BAEC were washed with phosphate-buffered saline and incubated for 10 min in lysis buffer (50 mM Tris-HCl, pH 7.4, 150 mM NaCl, 1% Nonidet P-40, 0.25% sodium deoxycholate, 1 mM EDTA, 2 mM Na_3VO_4, 1 mM NaF, 2 μg/ml leupeptin, 2 μg/ml antipain, 2 μg/ml soybean trypsin inhibitor, and 2 μg/ml lima trypsin inhibitor). Cells were harvested by scraping and centrifuged at 10,000 × *g* for 15 min at 4 °C. For immunoprecipitation, aliquots of cell homogenates were incubated with 12CA5 monoclonal antibody against the HA epitope (4 μg/ml) for 1 h at 4 °C. Protein G-Sepharose beads were added to the supernatant, incubated for 1 h, and washed extensively with lysis buffer. Bound immune complexes were eluted by boiling in Laemmli sample buffer, resolved by SDS-PAGE on 7.5% gels, and transferred onto nitrocellulose membranes. Immunoblots were probed with phospho-Ser^{1179}-eNOS, phospho-Ser^{116}-eNOS, eNOS, and HA epitope antibodies using protocols provided by the suppliers. For immunoblot analyses of cell lysates, 20 μg of cellular protein were resolved by SDS-PAGE, transferred to nitrocellulose membranes, and analyzed with phospho-Akt and Akt antibodies. Densitometric analyses of the immunoblots were performed using a ChemiImager 4000 (Alpha-Innotech).

In Vitro eNOS Phosphorylation—BAEC transfected with HA-tagged wild-type eNOS and myr$^-$ eNOS were harvested, lysed, and immunoprecipitated with anti-HA monoclonal antibody as described above. The immune complexes were isolated with protein G-Sepharose and incubated with active recombinant Akt (0.1–0.5 μg) in phosphorylation assay buffer (20 mM MOPS, pH 7.2, 25 mM β-glycerol phosphate, 5 mM EGTA, 1 mM sodium orthovanadate, 1 mM dithiothreitol) at 30 °C for 10 min. The reaction was stopped by adding 2× Laemmli sample buffer. Proteins were resolved by SDS-PAGE, transferred to nitrocellulose membranes, and probed with the phospho-Ser^{1179}-eNOS antibody.

Laser-scanning Confocal Microscopy—BAEC grown on coverslips were transfected at 50–60% confluency with plasmids encoding EGFP fusion constructs using FuGENE 6 reagent then incubated for 24 h to allow protein expression. The transfected cells were fixed using a 3.7% formaldehyde solution in phosphate-buffered saline and mounted on microscope slides with SlowFade® antifade kit (Molecular Probes, Inc.). Samples were imaged using a 60× differential interference contrast oil immersion objective lens on a Nikon E800 upright microscope with a Bio-Rad Radiance 2000 confocal attachment. Images are shown as single optical slices in the *z* axis.

RESULTS

We first studied the role of eNOS acyl modifications on agonist-induced eNOS phosphorylation at serine 1179, the putative site for agonist-modulated enzyme phosphorylation by kinase Akt (13, 16, 17, 21). We compared the phosphorylation pattern of wild-type eNOS and the eNOS acylation-deficient mutants in response to two different agonists known to promote the phosphorylation of eNOS on serine 1179, the polypeptide growth factor VEGF (16, 20) and the platelet-derived sphingolipid S1P (21). BAEC were transfected with cDNA encoding wild-type eNOS, myr$^-$ eNOS, or palm$^-$ eNOS, as described under "Experimental Procedures." Cells were treated

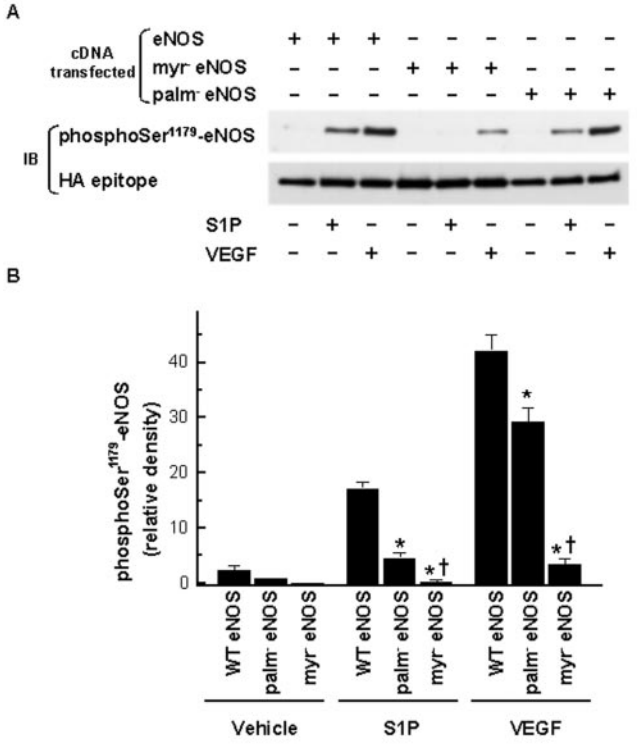

FIG. 1. **Agonist-induced serine 1179 phosphorylation in wild-type and acylation-deficient eNOS.** *Panel A* shows the results of immunoblot analyses prepared from BAEC transfected with cDNA encoding wild-type eNOS, myr$^-$ eNOS, and palm$^-$ eNOS, as indicated. Transfected cells were treated for 5 min with S1P (100 nM) or VEGF (1 nM). The recombinant proteins were immunoprecipitated with anti-HA epitope antibody, resolved by SDS-PAGE, and analyzed in immunoblots probed with antibodies against phospho-Ser^{1179}-eNOS or the HA epitope, as shown. This figure shows the results of a representative experiment that was repeated independently three times with equivalent results. *Panel B* shows the results of densitometric analyses from pooled data, plotting the degree of eNOS serine 1179 phosphorylation of wild-type and eNOS acylation mutants in basal conditions and after treatment with either S1P or VEGF. Each data point represents the mean ± S.E. derived from three independent experiments. The *asterisk* indicates $p < 0.05$ *versus* wild-type eNOS-transfected cells. The *dagger* indicates $p < 0.05$ *versus* palm$^-$ eNOS-transfected cells (analysis of variance).

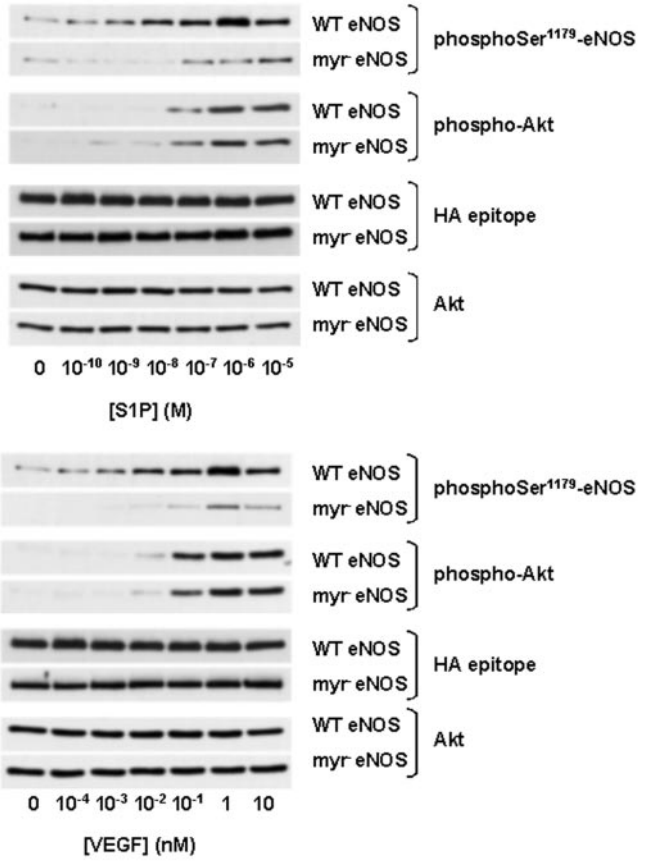

FIG. 2. **Dose response for agonist-mediated serine 1179 phosphorylation of wild-type and acylation-deficient eNOS.** BAEC transfected with cDNA encoding wild-type (*WT*) eNOS and myr$^-$ eNOS were treated with the indicated concentrations of S1P (*upper panel*) or VEGF (*lower panel*) for 5 min. The recombinant proteins were immunoprecipitated with the anti-HA epitope antibody, resolved by SDS-PAGE, and analyzed in immunoblots probed with phospho-Ser^{1179}-eNOS antibody. Equal loading of samples was confirmed by re-probing the immunoblots with HA epitope polyclonal antibody (*lower lanes* in each *panel*). In parallel, cell lysates (20 μg/lane) were resolved by SDS-PAGE and analyzed by immunoblotting with phospho-Akt and Akt antibodies. Shown are the representative results of an experiment that was repeated three times with equivalent results.

with S1P (100 nM) or VEGF (1 nM) for 5 min, and the recombinant proteins were immunoprecipitated with the anti-HA epitope antibody. eNOS phosphorylation at serine 1179 was analyzed in immunoblots probed with a phospho-specific antibody. As shown in Fig. 1, wild-type eNOS was robustly phosphorylated at serine 1179 in response to S1P and VEGF stimulation. However, S1P-induced serine 1179 phosphorylation of the myr$^-$ eNOS was completely abrogated, whereas the response to VEGF was reduced by 91 ± 3% ($n = 3, p < 0.01$) in the myr$^-$ eNOS. An intermediate phenotype was found for the palm$^-$ eNOS: S1P-induced serine 1179 phosphorylation was reduced by 72 ± 7% ($n = 3, p < 0.01$), and there was a 30 ± 9% decrease ($n = 3, p < 0.05$) in the serine 1179 phosphorylation in response to VEGF.

We next analyzed the time course and dose response for S1P- and VEGF-induced serine 1179 phosphorylation in wild-type and myr$^-$ eNOS. As seen in Fig. 2, both agonists stimulated a dose-dependent increase in serine 1179 eNOS phosphorylation of the wild-type enzyme, with EC_{50} values of 10 nM and 0.01 nM for S1P and VEGF, respectively. The phosphorylation of myr$^-$ eNOS at serine 1179 was attenuated even at the highest agonist doses (Fig. 2). As shown in Fig. 3, S1P and VEGF exhibited a similar time course for agonist-induced phosphorylation of wild-type eNOS at serine 1179, but the myr$^-$ eNOS showed markedly attenuated phosphorylation at all time points in response to these agonists. As shown in Figs. 2 and 3, agonist-induced phosphorylation of kinase Akt was unaffected by transfection of the different eNOS constructs; loading controls showed equivalent levels of protein expression under these different experimental conditions. We next used purified kinase Akt to explore whether there was an intrinsic difference between the wild-type and myr$^-$ eNOS in their suitability as a substrate for this kinase. As shown in Fig. 4, both the wild-type and myr$^-$ eNOS served as effective substrates for *in vitro* phosphorylation by kinase Akt, with identical dose responses and time courses of Akt-induced phosphorylation. The control experiments shown in Fig. 4 established the specificity both of the phosphoserine 1179 antibody as well as the immunoprecipitation of recombinant eNOS using the HA epitope tag; for the S1179A eNOS mutant, in which the putative Akt phosphorylation site at serine 1179 was changed to alanine, there was no phosphorylation whatsoever when this immunoprecipitated mutant eNOS was incubated with purified kinase Akt.

To more fully understand the effects of eNOS targeting on enzyme phosphorylation, we next analyzed a series of chimeric eNOS proteins in which the transmembrane domain of the cell surface glycoprotein CD8 was fused either to the myr$^-$ eNOS or

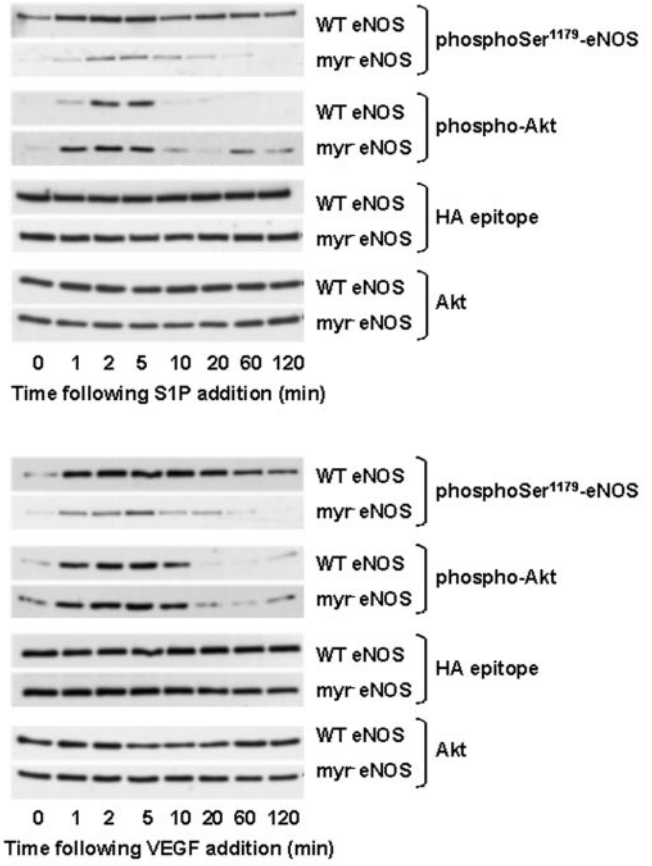

FIG. 3. **Time course of S1P- and VEGF-induced serine 1179 phosphorylation in wild-type and acylation-deficient eNOS.** BAEC transfected with cDNA encoding wild-type (*WT*) eNOS and myr$^-$ eNOS were treated with S1P (100 nM, *upper panel*) or VEGF (1 nM, *lower panel*) for the indicated times. Recombinant proteins were immunoprecipitated with the anti-HA epitope antibody, and the immune complexes were resolved by SDS-PAGE and analyzed in immunoblots probed with phospho-Ser^{1179}-eNOS and anti-HA epitope polyclonal antibody, as noted. In parallel, cell lysates (20 μg/line) were resolved by SDS-PAGE, transferred to nitrocellulose, and immunoblotted with phospho-Akt and Akt antibodies. These experiments were repeated three times with equivalent results.

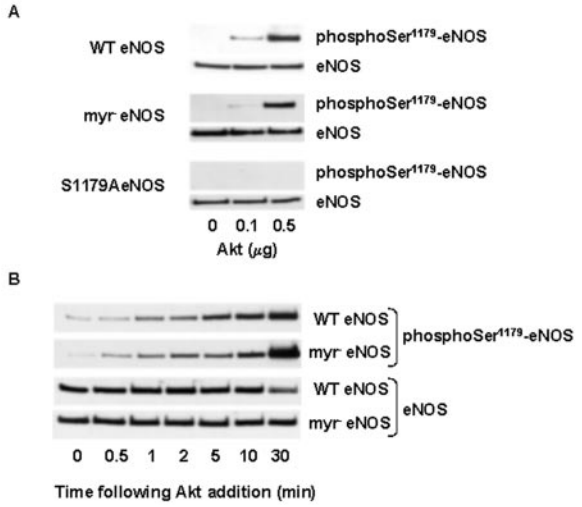

FIG. 4. ***In vitro* phosphorylation of wild-type and acylation-deficient eNOS by kinase Akt.** BAEC transfected with wild-type (*WT*) eNOS, myr$^-$ eNOS, and S1179AeNOS were lysed, and recombinant eNOS was immunoprecipitated with anti-HA epitope antibody and analyzed in a kinase activity assay as described under "Experimental Procedures." In *panel A*, immunoprecipitates were incubated with the indicated amounts of purified recombinant active Akt for 10 min, and the reaction mixture was resolved by SDS-PAGE, transferred to nitrocellulose membranes, and probed with phospho-Ser^{1179}-eNOS antibody. Equal loading of samples was confirmed by re-probing the immunoblots with eNOS antibody. These experiments were repeated twice with equivalent results. *Panel B* shows the time course for *in vitro* phosphorylation of wild-type eNOS and myr$^-$ eNOS by Akt. Wild-type eNOS and myr$^-$ eNOS immunoprecipitated with anti-HA epitope antibody from BAEC lysates were incubated with 0.25 μg of recombinant Akt for the indicated times. Reaction mixtures were resolved by SDS-PAGE, and eNOS phosphorylation was analyzed in immunoblots probed with the phospho-Ser^{1179}-eNOS antibody. Equal loading was confirmed by re-probing the membranes with eNOS antibody.

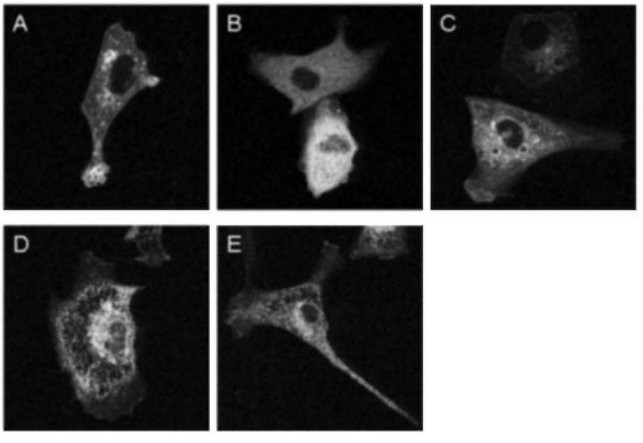

FIG. 5. **Subcellular distribution of EGFP-labeled wild-type, chimeric, and acylation-deficient eNOS constructs.** The images shown are representative laser scanning confocal photomicrographs of BAEC transfected with eNOS-EGFP (*A*), myr$^-$eNOS-EGFP (*B*), palm$^-$ eNOS-EGFP (*C*), CD8·myr$^-$ eNOS-EGFP (*D*), or CD8·myr$^-$ palm$^-$ eNOS-EGFP (*E*). The images are representative of 24–100 images analyzed in 4–10 independent experiments for each sample.

to the myr$^-$/palm$^-$ eNOS (8). We have previously used biochemical approaches to explore features of the acylation and targeting of these chimeras (8). As shown in Fig. 5, we used here cellular imaging methodologies to further characterize the subcellular distribution of these CD8.eNOS chimeras by first fusing these constructs at their carboxyl termini to the green fluorescent protein EGFP and then performing laser scanning confocal microscopy on BAEC transfected with these plasmids. The subcellular distribution of these various EGFP-tagged eNOS constructs, wild-type eNOS (*panel A*), myr$^-$ mutant eNOS (*panel B*), palm$^-$ mutant eNOS (*panel C*), or the CD8 fusion constructs ligated to myr$^-$ eNOS (*panel D*) or to myr$^-$ palm$^-$ mutant eNOS (*panel E*), revealed distinctive patterns (Fig. 5). The wild-type eNOS-EGFP fusion protein targeted to peripheral as well as intracellular membranes. By contrast, the myr$^-$-EGFP fusion protein showed a diffuse intracellular pattern, consistent with prior reports that used biochemical (7) and imaging (28) approaches. The palmitoylation-deficient eNOS-EGFP fusion protein had a pattern of intracellular distribution similar to the wild type, but there was less uniform staining of the peripheral cell membrane in the palm$^-$ mutant enzyme compared with wild-type eNOS (Fig. 5*C*). The addition of the CD8 transmembrane domain rescued the phenotype of the myr$^-$ and palm$^-$ mutants, restoring membrane targeting to yield a pattern similar to that of the wild-type eNOS-EGFP protein.

Having confirmed a similar subcellular distribution for wild-type eNOS and the CD8-eNOS chimeras, we next studied the agonist-induced phosphorylation pattern of these constructs in transfected BAEC. As shown in Fig. 6, the CD8.myr$^-$ eNOS and CD8.myr$^-$ palm$^-$ eNOS chimeras showed a similar pattern of S1P- or VEGF-induced phosphorylation at serine 1179. The time course of agonist-induced serine 1179 phosphoryla-

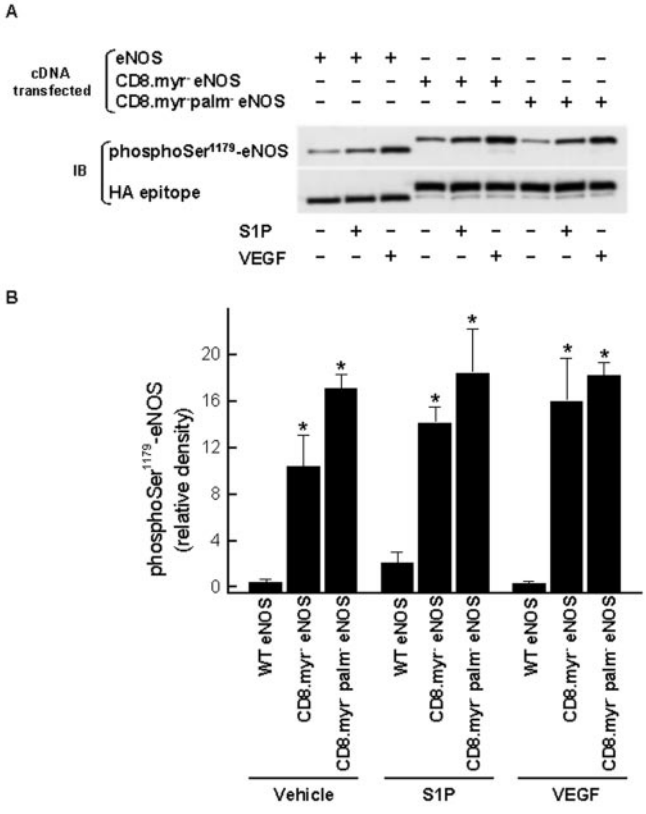

FIG. 6. **Agonist-induced serine 1179 phosphorylation of CD8.eNOS chimeric constructs.** In *panel A*, BAEC transfected with cDNA encoding wild-type eNOS, CD8.myr$^-$ eNOS, or CD8.myr$^-$ palm$^-$ eNOS (as indicated) were treated for 5 min with S1P (100 nM) or VEGF (1 nM). Recombinant proteins were immunoprecipitated with HA epitope antibody, resolved by SDS-PAGE, and analyzed in immunoblots (*IB*) probed with the phospho-Ser^{1179}-eNOS antibody. Equal loading of the samples was validated by re-probing the immunoblots with anti-HA epitope polyclonal antibody. Shown are the results from a representative experiment that was repeated independently four times with equivalent results. *Panel B* shows the result of the densitometric analyses from pooled data, plotting the degree of serine 1179 phosphorylation for wild-type (*WT*) eNOS and chimeric constructs after vehicle, S1P, or VEGF treatment, as indicated. Each data point represents the mean ± S.E. derived from four independent experiments. The *asterisk* indicates a difference at $p < 0.05$ *versus* basal phosphorylation.

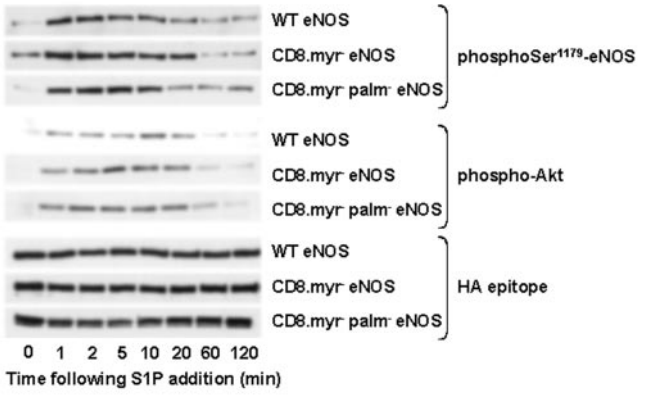

FIG. 7. **Time course of S1P-induced serine 1179 phosphorylation of wild-type and CD8.eNOS constructs.** BAEC transfected with cDNA encoding wild-type (*WT*) eNOS, CD8.myr$^-$ eNOS, or CD8.myr$^-$ palm$^-$ eNOS were treated with 100 nM S1P for the indicated times. Recombinant proteins were immunoprecipitated with anti-HA epitope antibody, and the immune complexes were resolved by SDS-PAGE and analyzed in immunoblots probed with phospho-Ser^{1179}-eNOS and HA epitope tag antibodies, as indicated. In parallel, cell lysates (20 μg/line) were resolved by SDS-PAGE, transferred to nitrocellulose, and immunoblotted with phospho-Akt antibody. These experiments were repeated three times with equivalent results.

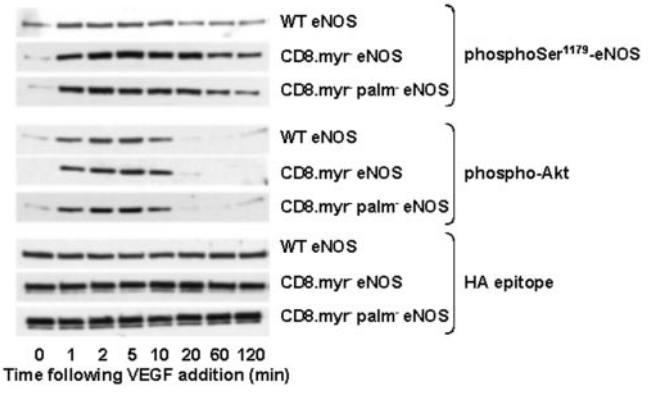

FIG. 8. **Time course of VEGF-induced serine 1179 phosphorylation of wild-type and CD8.eNOS constructs.** BAEC transfected with cDNA encoding wild-type (*WT*) eNOS, CD8.myr$^-$ eNOS, or CD8.myr$^-$ palm$^-$ eNOS were treated with 1 nM VEGF for the indicated times. Recombinant proteins were immunoprecipitated with the anti-HA epitope antibody, and immune complexes were resolved by SDS-PAGE and analyzed in immunoblots probed with phospho-Ser^{1179}-eNOS or HA tag antibodies, as indicated. In parallel, cell lysates (20 μg/line) were resolved by SDS-PAGE, transferred to nitrocellulose, and immunoblotted with the phospho-Akt antibody. The results shown are representative of experiments that were repeated three times with equivalent results.

tion was identical for these various constructs for both S1P (Fig. 7) and VEGF (Fig. 8). For both agonists, the time course of eNOS phosphorylation at serine 1179 coincided with the temporal pattern of agonist-induced kinase Akt phosphorylation; loading controls verified equivalent protein recovery under these different experimental treatments (Figs. 7 and 8). The phosphoinositide 3-kinase inhibitor wortmannin completely blocked the phosphorylation of kinase Akt and abrogated the serine 1179 phosphorylation of both the wild-type eNOS and the CD8-eNOS chimeric constructs (Fig. 9).

In our final series of experiments, we explored the effects of eNOS acylation on the phosphorylation of eNOS on serine 116, a site that is phosphorylated in BAEC (13, 14) and for which a phospho-specific antibody has recently been validated (14). We transfected BAEC with a series of eNOS constructs, including the wild-type enzyme, the acylation-deficient mutants, and the CD8.eNOS chimeric constructs described above. The recombinant proteins were immunoprecipitated using anti-HA epitope antibody, and eNOS phosphorylation at serine 116 was analyzed by immunoblotting with an antibody specific for phosphorylation at this site (14). As shown in Fig. 10 and as expected from our previous work (14), wild-type eNOS was phosphorylated at serine 116. Strikingly, the myr$^-$ mutant showed substantively enhanced phosphorylation at serine 116; as noted above, this same mutant exhibited a marked reduction in phosphorylation at serine 1179 (Figs. 1–3). In contrast to the myr$^-$ mutant, the CD8 eNOS fusion proteins showed a significant reduction in serine 116 phosphorylation compared with the wild-type protein (Fig. 10). Taken together, these results suggest that, in direct contrast to the membrane-association requirement for serine 1179 phosphorylation, the phosphorylation of eNOS on serine 116 is enhanced when the enzyme is present in the cytosol and is attenuated when eNOS is membrane-targeted.

DISCUSSION

This study provides several new lines of evidence that agonist-induced phosphorylation of eNOS at serine 1179 by kinase Akt is largely restricted to the membrane-targeted form of the enzyme and importantly extends recent observations (14, 29).

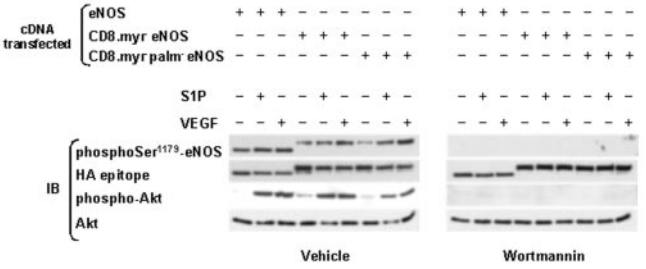

FIG. 9. **Effects of wortmannin on agonist-induced serine 1179 phosphorylation of wild-type eNOS and chimeric constructs.** BAEC were transfected with wild-type eNOS, CD8.myr$^-$ eNOS, or CD8.myr$^-$ palm$^-$ eNOS, as noted. Before the addition of S1P (100 nM for 5 min) or VEGF (1 nM for 5 min), BAEC were treated with 1 μM wortmannin or vehicle for 30 min. Recombinant proteins were immunoprecipitated with the anti-HA epitope antibody and resolved by SDS-PAGE, and immunoblots (*IB*) were probed with phospho-Ser^{1179}-eNOS antibody. Equal loading of the samples were confirmed by re-probing the immunoblots with anti-HA epitope antibody. In parallel, cell lysates (20 μg/lane) from BAEC were resolved by SDS-PAGE and probed with phospho-Akt and Akt antibodies. These results are representative of two independent experiments.

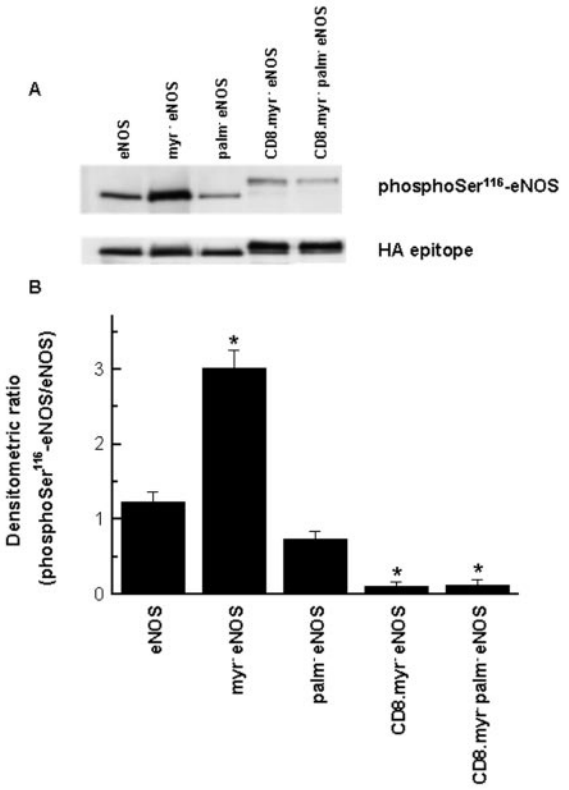

FIG. 10. **Serine 116 phosphorylation of wild-type eNOS, acylation-deficient eNOS, and CD8.eNOS chimeras.** *Panel A* shows a representative immunoblot probed with the anti-phosphoserine 116 eNOS antibody, analyzed in BAEC transfected with cDNA encoding wild-type eNOS or eNOS acylation-deficient/chimeric constructs, as shown. The recombinant proteins were immunoprecipitated with the anti-HA epitope antibody, and immune complexes were resolved by SDS-PAGE and analyzed in immunoblots probed, as indicated, with antibodies against phospho-Ser^{116}-eNOS or the HA epitope (as a loading control). Shown are the results from a representative experiment that was repeated three times with equivalent results. *Panel B* shows the result of densitometric analyses from pooled data, plotting the degree of serine 116 phosphorylation of wild-type eNOS, eNOS acylation-deficient mutants, and chimeric proteins, as normalized to the total expression of recombinant protein for each construct (determined using the antibody against the HA epitope). Each data point represents the mean ± S.E. derived from three independent experiments. The *asterisk* notes $p < 0.05$ *versus* wild-type eNOS-transfected cells (analysis of variance).

An acylation-deficient eNOS mutant (myr$^-$ eNOS) shows virtually no basal or agonist-induced phosphorylation at serine 1179 in response to either the polypeptide growth factor VEGF or the sphingolipid S1P (Fig. 1). By contrast, the wild-type eNOS shows marked phosphorylation in response to VEGF, with the effects of S1P being slightly less robust (Figs. 1–3). The wild-type and acylation-deficient eNOS mutants serve equally effectively as substrates for protein kinase Akt *in vitro* (Fig. 4), suggesting that it is the subcellular localization of these proteins rather the direct effects of eNOS acylation that differentiate the wild-type and mutant proteins. We may further conclude that membrane targeting and not acylation *per se* represents that key determinant of eNOS phosphorylation at serine 1179; ligation of the CD8 transmembrane domain to an acylation-deficient eNOS mutant fully rescues the phenotype of the wild-type enzyme in terms of both its subcellular localization (Fig. 5) and serine 1179 phosphorylation (Figs. 6–8).

The palm$^-$ eNOS mutant shows an intermediate phenotype for agonist-induced phosphorylation at serine 1179 (Fig. 1), consistent with our previous observations that the palm$^-$ mutant is less effectively targeted to the membrane fraction (Ref. 5; see also Fig. 5). Palmitoylation of eNOS facilitates the targeting of the enzyme to plasmalemmal caveolae (30), and prolonged agonist treatment of endothelial cells promotes eNOS depalmitoylation (6) and translocation of the enzyme from peripheral to internal membrane fractions (31). Our finding that eNOS undergoes differential phosphorylation depending upon its subcellular targeting may thus directly relate to the control of pathways that modulate the endogenous cycle of reversible eNOS depalmitoylation and translocation seen with agonist treatment. The fact that the palmitoylation-deficient eNOS shows attenuated agonist-dependent serine 1179 phosphorylation is consistent with the hypothesis that eNOS depalmitoylation helps to promote deactivation of the enzyme. Interestingly, the palmitoylation-deficient mutant eNOS is indistinguishable from wild-type eNOS in its phosphorylation at serine 116. Further study will be required to discern whether the dynamic regulation of serine 116 phosphorylation is altered in the palmitoylation-deficient mutant.

The level of phosphorylation of a protein at a given residue reflects, of course, the balance of protein kinase and phosphoprotein phosphatase activities at that site. It is therefore not clear whether the enhanced phosphorylation of membrane-targeted eNOS at serine 1179 reflects more the inability of a cytosolic phosphatase to dephosphorylate the phosphoenzyme, the enhanced ability of a membrane-associated kinase to phosphorylate the enzyme, or both. The inverse may be true for phosphorylation at serine 116, but the paucity of information about the relevant kinase at the serine 116 site hinders further speculation. However, kinase Akt, which has been convincingly implicated in eNOS phosphorylation at serine 1179 (Refs. 16 and 17; see Fig. 4) is known to be principally a cytosolic enzyme (32, 33). Kinase Akt transiently targets to the membrane to be activated, and the activated kinase has important targets in the cytosol and the nucleus (32–35). Furthermore, kinase pathways upstream from kinase Akt are membrane-associated (36). Robust eNOS phosphorylation could require only that a small fraction of the total cellular Akt kinase is associated with the plasmalemmal caveolae in which eNOS resides. Alternatively, an active phosphoprotein phosphatase present in the cytosol could be responsible for the weak eNOS phosphorylation on serine 1179 that is seen with the myr$^-$ mutant eNOS. Indeed, the time course for the return of maximal levels of agonist-induced serine 1179 phosphorylation down to basal levels parallels the time course observed in BAEC for agonist-induced translocation from peripheral to internal membranes and back

again (31, 37). It must be noted, however, that the fully acylation-deficient CD8.eNOS chimeras exhibit time courses and dose responses for agonist-induced serine 1179 phosphorylation and dephosphorylation that are identical to the wild-type enzyme (Figs. 7 and 8). The latter observations suggest that the relevant serine 1179 kinase(s) and phosphatase(s) are fully able to modify membrane-associated eNOS independent of its reversible acylation.

eNOS phosphorylation at serine 116 shows striking differences from the pattern of phosphorylation at serine 1179. As shown in Fig. 10, the myr$^-$ mutant, which is restricted to the cytosol and exhibits significantly attenuated serine 1179 phosphorylation, consistently shows markedly enhanced phosphorylation at serine 116. Consistent with this observation, the CD8-eNOS fusion proteins, which are exclusively membrane-targeted, exhibit an attenuated level of serine 116 phosphorylation compared with the wild-type enzyme (Fig. 10). We have previously reported that the VEGF-induced dephosphorylation of eNOS on serine 116 appears to involve a pathway mediated by the calcium-activated phosphatase calcineurin (14), but the protein kinase involved in phosphorylation at this site has not been identified. Calcineurin is principally a cytosolic protein but can rapidly associate with cell membranes by virtue of its specific association with membrane-targeted signaling protein complexes (38, 39). With the available data, we cannot discern whether it is the enhanced activity of an unknown soluble kinase, the reduced activity of a membrane-targeted phosphatase, or both that are responsible for the exaggerated phosphorylation of eNOS on serine 116 when the enzyme is present in the cell cytosol. These observations do allow us to conclude that the phosphorylation of eNOS on discrete sites is differentially affected by the subcellular targeting of the enzyme and to suggest that the inter-relationships of eNOS acylation and phosphorylation may have important implications for regulation of NO-dependent signaling pathways in the vascular wall.

Acknowledgments—We acknowledge the contributions of Drs. Hongjie Chen and Junsuke Igarashi for many helpful suggestions in the execution of this work.

REFERENCES

1. Moncada, S., and Higgs, A. (1993) *N. Engl. J. Med.* **329,** 2002–2012
2. Loscalzo, J., and Welch, G. (1995) *Prog. Cardiovasc. Dis.* **38,** 87–104
3. Michel, T., and Feron, O. (1997) *J. Clin. Invest.* **100,** 2146–2152
4. Shaul, P. W., and Anderson, R. G. (1998) *Am. J. Physiol.* **275,** L843–L851
5. Robinson, L. J., and Michel, T. (1995) *Proc. Natl. Acad. Sci. U. S. A.* **92,** 11776–11780
6. Robinson, L. J., Busconi, L., and Michel, T. (1995) *J. Biol. Chem.* **270,** 995–998
7. Busconi, L. and Michel, T. (1993) *J. Biol. Chem.* **268,** 8410–8413
8. Prabhakar, P., Cheng, V., and Michel, T. (2000) *J. Biol. Chem.* **275,** 19416–19421
9. Kantor, D. B., Lanzrein, M., Stary, S. J., Sandoval, G. M., Smith, W. B., Sullivan, B. M., Davidson, N., and Schuman, E. M. (1996) *Science* **274,** 1744–1748
10. Feron, O., Michel, J. B., Sase, K., and Michel, T. (1998) *Biochemistry* **37,** 193–200
11. Ghosh, S., Gachhui, R., Crooks, C., Wu, C., Lisanti, M. P., and Stuehr, D. J. (1998) *J. Biol. Chem.* **273,** 22267–22271
12. Michel, T., Li, G. T., and Busconi, L. (1993) *Proc. Natl. Acad. Sci. U. S. A.* **90,** 6252–6256
13. Gallis, B., Corthals, G. L., Goodlett, D. R., Kim, H. U. F., Presnell, S. R., Figeys, D., Harrison, D. G., Berk, B. C., Aebersold, R., and Corson, M. A. (1999) *J. Biol. Chem.* **274,** 30101–30108
14. Kou, R., Greif, D., and Michel, T. (2002) *J. Biol. Chem.* **277,** 29669–29673
15. Harris, M. B., Venema, V. J., Liang, H., Zou, R., Michell, B. J., Chen, Z. P., Kemp, B. E., and Venema, R. C. (2001) *J. Biol. Chem.* **276,** 16587–16591
16. Fulton, D., Gratton, J. P., McCabe, T. J., Fontana, J., Fujio, Y., Walsh, K., Franke, T. F., Papapetropoulos, A., and Sessa, W. C. (1999) *Nature* **399,** 597–601
17. Dimmeler, S., Fleming, I., Fisslthaler, B., Hermann, C., Busse, R., and Zeiher, A. M. (1999) *Nature* **399,** 601–605
18. Chen, Z. P., Mitchelhill, K. I., Michell, B. J., Stapleton, D., Rodriguez-Crespo, I., Witters, L. A., Power, D. A., Ortiz de Montellano, P. R., and Kemp, B. E. (1999) *FEBS Lett.* **43,** 285–289
19. Butt, E, Bernhardt, M., Smolenski, A., Kotsonis, P., Fröhlich, L. G., Sickmann, A., Meyer, H. E., Lohmann, S. M., and Schmidt, H. H. H. W. (2000) *J. Biol. Chem.* **275,** 5179–5187
20. Michell, B. J., Griffiths, J. E., Mitchelhill, K. I., Rodriguez-Crespo, I., Tiganis, T., Bozinovski, S., de Montellano, P. R., Kemp, B. E., and Pearson, R. B. (1999) *Curr. Biol.* **9,** 845–848
21. Igarashi, J., Bernier, S. G., and Michel, T. (2001) *J. Biol. Chem.* **276,** 12420–12426
22. Montagnani, M., Chen, H., Barr, V. A., and Quon, M. J. (2001) *J. Biol. Chem.* **276,** 30392–30398
23. Kou, R., Igarashi, J., and Michel, T. (2002) *Biochemistry* **41,** 4982–4988
24. Hisamoto, K., Ohmichi, M., Kurachi, H., Hayakawa, J., Kanda, Y., Nishio, Y., Adachi, K., Tasaka, K., Miyoshi, E., Fujiwara, N., Taniguchi, N., and Murata, Y. (2001) *J. Biol. Chem.* **276,** 3459–3467
25. Fleming, I., Fisslthaler, B., Dimmeler, S., Kemp, B. E., and Busse, R. (2001) *Circ. Res.* **88,** 68–75
26. Bernier, S. G., Haldar, S., and Michel T. (2000) *J. Biol. Chem.* **275,** 30707–30715
27. Lee, H., Goetzl, E. J., and An, S. (2000) *Am. J. Physiol. Cell Physiol.* **278,** 612–618
28. Liu, J., Hughes, T. E., and Sessa, W. C. (1997) *J. Cell Biol.* **137,** 1525–1535
29. Fulton, D., Fontana, J., Sowa, G., Gratton, J. P., Lin, M., Li, K. X., Michell, B., Kemp, B. E., Rodman, D., and Sessa W. C. (2002) *J. Biol. Chem.* **277,** 4277–4284
30. Shaul, P. W., Smart, E. J., Robinson, L. J., German, Z., Yuhanna, I. S., Ying, Y., Anderson, R. G., and Michel, T. (1996) *J. Biol. Chem.* **271,** 6518–6522
31. Prabhakar, P., Thatte, H. S., Goetz, R. M., Cho, M. R., Golan, D. E., and Michel, T. (1998) *J. Biol. Chem.* **273,** 27383–27388
32. Kandel, E. S., and Hay, N. (1999) *Exp. Cell Res.* **253,** 210–229
33. Brazil, D. P., and Hemmings, B. A. (2001) *Trends Biochem. Sci.* **26,** 657–664
34. Meier, R., Alessi, D. R., Cron, P., Andjelkovic, M., and Hemmings, B. A. (1997) *J. Biol. Chem.* **272,** 30491–30497
35. Astoul, E., Watton, S., and Cantrell, D. (1999) *J. Cell Biol.* **145,** 1511–1520
36. Vanhaesebroeck, B., and Alessi, D. R. (2000) *Biochem. J.* **346,** 561–576
37. Goetz, R. M., Thatte, H. S., Prabhakar, P., Cho, M. R., Michel, T., and Golan, D. E. (1999) *Proc. Natl. Acad. Sci.* **96,** 2788–2793
38. Klauck, T. M., Faux, M. C., Labudda, K., Langeberg, L. K., Jaken, S., and Scott, J. D. (1996) *Science* **271,** 1589–1592
39. Sim, A. T., and Scott, J. D. (1999) *Cell Calcium* **26,** 209–217